Research Square

Preprints are preliminary reports that have not undergone peer review.
They should not be considered conclusive, used to inform clinical practice,
or referenced by the media as validated information.

Hysteretic foundation softening and the tuning of tuned mass dampers in frames on soil: is adaptive retuning worth it?

Seyyed Mostafa Razavi

s.m.razavi@mshdiau.ac.ir

Islamic Azad University, Mashhad

Aida Rahmati

University of Shahrood

Research Article

Keywords: Tuned mass damper, Soil–structure interaction, Hysteretic foundation, Bouc–Wen model, Adaptive tuning, Moment frame

Posted Date: November 18th, 2026

DOI: https://doi.org/10.21203/rs.3.rs-11336344/v1

License: This work is licensed under a Creative Commons Attribution 4.0 International License.
Read Full License

Additional Declarations: No competing interests reported.

Hysteretic foundation softening and the tuning of tuned mass dampers in frames on soil: is adaptive retuning worth it?

Seyed Mostafa Razavi[1]*, Aida Rahmati[2]

[1] Faculty of Engineering, Mashhad Branch, Islamic Azad University, Mashhad, Iran

[2] Faculty of Engineering, Shahrood University of Technology, Shahrood, Iran

* Corresponding author: s.m.razavi@mshdiau.ac.ir

Abstract Tuned mass dampers (TMDs) are tuned to a single frequency, yet strong shaking can soften the soil–foundation interface and lengthen the period of a frame while the earthquake is in progress. This study quantifies how much hysteretic foundation softening detunes a roof-mounted TMD and whether adaptive retuning is worth its added complexity. Two shear-type frames (7 and 11 storeys) are placed on a Bouc–Wen horizontal–rocking foundation macro-element on two soil classes and subjected to stochastic Kanai–Tajimi ground motions scaled to 0.2 g and 0.5 g (eight cases, five test motions each). Five TMD designs with the same 2% mass ratio are compared: tuning to the fixed-base frequency, tuning to the small-strain soil–structure frequency, a passive design optimised on training motions, an adaptive variable-stiffness TMD that estimates the system frequency from noisy roof acceleration, and the same device with the exact frequency. The secant-window frequency of the system fell by 3% to 32%, and in the reference case a TMD tuned to the small-strain frequency was detuned by more than 10% during 64% of the record. Even so, tuning to the soil–structure frequency rather than the fixed-base frequency increased the reduction of peak roof displacement by 7.2 percentage points on average, whereas adaptive retuning changed it by -1.3 points with the estimated frequency and +0.1 points with the exact frequency, relative to the small-strain tuning. In these models, soil-aware passive tuning captures most of the benefit. The conclusions are limited by synthetic ground motions and two frames.

Keywords: Tuned mass damper; Soil–structure interaction; Hysteretic foundation; Bouc–Wen model; Adaptive tuning; Moment frame

1 Introduction

A tuned mass damper (TMD) reduces structural vibration by transferring energy to an auxiliary oscillator tuned to a target frequency of the structure [1]. Its effect is well established for narrow-band loading such as wind. Under earthquakes the excitation is broadband and non-stationary and the structural frequency is uncertain, which makes tuning more delicate. Tuning rules and parametric studies for seismic applications [2, 3] give the frequency and damping ratios to use for a given mass ratio.

Soil flexibility lengthens the period of a structure and changes its damping [4–6], so the frequency to which a TMD should be tuned is not the fixed-base frequency. Random-vibration studies reported that strong soil–structure interaction (SSI) reduces the effectiveness of TMDs because of the high damping of the soil–

structure system on soft soil [7]. Centrifuge tests found that tuning a TMD to the properties of the soil–structure system, instead of the fixed-base properties, doubled the improvement in damping [8]. Non-dimensional performance curves later identified the structure-to-soil stiffness ratio and the parameters governing foundation rocking as the main controls of TMD effectiveness [9]. Multiple TMDs [10], parameter optimisation [11] and active control [12] have also been studied for soil–structure systems.

Most of these studies describe the soil by linear, possibly frequency-dependent, springs and dashpots. In strong shaking the soil–foundation interface yields, the horizontal and rocking stiffness decrease, and the period of the system lengthens while the earthquake is in progress. Studies that include nonlinear soil behaviour have used passive TMDs on beam-on-nonlinear-Winkler foundations [13] and semi-active TMDs with variable damping on nonlinear soil–pile models [14]. Variable-stiffness semi-active TMDs have been designed for nonlinear structures with a cone-model representation of the soil [15], and an adaptive-passive TMD has been proposed for aseismic protection including SSI [16]. Variable stiffness and adaptive tuning are older ideas in structural control [17, 18].

Three questions remain open in the studies reviewed here. First, how large is the softening of the soil–foundation interface under strong shaking, and how far does it detune a TMD tuned in the conventional way? Second, is the benefit of retuning measured against a passive TMD that has already been tuned to the soil–structure system, and not only against one tuned to the fixed-base frame? Third, does the benefit survive when the frequency has to be estimated from noisy sensor data and applied through an actuator with lag and limits?

This paper addresses these questions with a coupled frame–hysteretic foundation–TMD model. The contributions are: (i) a model in which the foundation softens through Bouc–Wen springs, with an instantaneous detuning index based on the tangent and secant-window frequencies of the system; (ii) a quantification of the softening for two frames, two soils and two shaking intensities; (iii) a paired comparison of five TMD designs, including a passive design tuned to the soil–structure frequency and an adaptive device with realistic estimation noise and actuator limits, together with an exact-frequency upper bound; and (iv) the finding, for these models, that soil-aware passive tuning captures most of the benefit and adaptive retuning adds none that can be measured.

Section 2 presents the model, Section 3 the TMD designs, Section 4 the case studies, Section 5 the verification, Section 6 the results, Section 7 the discussion and limitations, and Section 8 the conclusions.

2 Coupled soil–frame–TMD model

2.1 Superstructure

The superstructure is a planar shear-type frame with n storeys, with lumped floor masses m_i and storey stiffnesses k_i taken from the authors' earlier work [19] (Section 4.1). The 11-storey frame follows a model from the literature [12]. The stiffness matrix K_s of the shear building is assembled from the storey

stiffnesses, and Rayleigh damping of 2% is assigned in the first two fixed-base modes. The complete model, with the frame, the rigid foundation block with its two hysteretic springs and dashpots, and the roof TMD, is shown in Fig. 1.

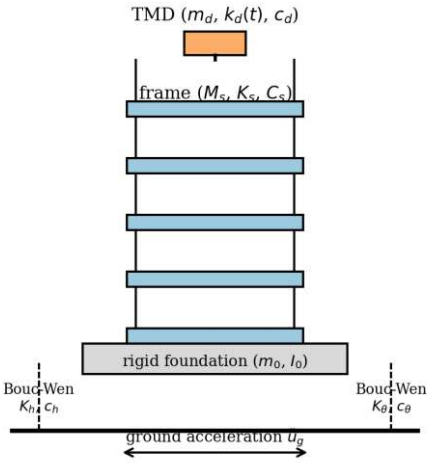


Fig. 1. *Coupled soil–frame–TMD model.*

2.2 Foundation macro-element

The foundation is a rigid block with mass m_0 and rotational inertia I_0, with horizontal translation u_0 and rocking θ relative to the free field. Each degree of freedom has a hysteretic spring in parallel with a radiation dashpot:

$$F_h = \alpha_h K_h u_0 + (1-\alpha_h) K_h u_y z_h + c_h \dot{u}_0 \qquad (1)$$

$$M_f = \alpha_\theta K_\theta \theta + (1-\alpha_\theta) K_\theta \theta_y z_\theta + c_\theta \dot{\theta} \qquad (2)$$

The dimensionless hysteretic variable z follows the Bouc–Wen equation [20, 21] with $A = 1$ and $n = 1$,

$$\dot{z} = \frac{1}{u_y}\left[\dot{u} - \beta\,|\dot{u}|\,z - \gamma\,\dot{u}\,|z|\right] \qquad (3)$$

where u and u_y are replaced by θ and θ_y for the rocking spring, and $\beta = \gamma = 0.5$. K_h and K_θ are the small-strain stiffnesses, α the post-yield stiffness ratio (0.05), and u_y and θ_y the yield sway and rotation. The stiffness and dashpot coefficients of the soft soil are those of the earlier work [19], obtained from the relations of Wolf [22]. Uplift, horizontal–rocking coupling and pile effects are not modelled.

2.3 Tuned mass damper

A roof TMD with mass m_d, stiffness k_d and damping c_d is attached to the top floor. The mass ratio is $\mu = m_d/\Sigma m_i$, the damper frequency is $\omega_d = (k_d/m_d)^{1/2}$ and the damping ratio is $\zeta_d = c_d/(2m_d\omega_d)$. For the adaptive device k_d varies in time (Section 3).

2.4 Equations of motion

The generalised coordinates are $q = [u_0, \theta, u_1, \ldots, u_n, u_d]^T$, where u_i are the floor deformations relative to the rigidly rotating foundation block and u_d is the TMD displacement relative to the roof. The equations of motion are

$$M\,\ddot{q} + C\,\dot{q} + K(t)\,q + f_f(q,z) = -p\,\ddot{u}_g \qquad (4)$$

where M contains the kinematic coupling between sway, rocking and the floor masses, $K(t)$ contains the frame stiffness and the time-varying TMD stiffness, f_f collects the foundation forces of Eqs. (1) and (2), p is the influence vector and $\ddot{u}_g$ is the ground acceleration. Matrices and vectors are written in italic. Equation (4) is solved together with Eq. (3) for both springs and with the actuator equation of k_d (Section 3.3) as a first-order system, using the LSODA solver of SciPy with a sampling step of 0.01 s.

2.5 Instantaneous frequencies and detuning index

For a single-degree-of-freedom structure of stiffness k and height h on a flexible base, the effective period is [4]

$$\tilde{T} = T\sqrt{1 + \frac{k}{K_h} + \frac{kh^2}{K_\theta}} \qquad (5)$$

Two instantaneous frequencies of the system without the TMD are used. The tangent frequency $\omega_t(t)$ is the lowest eigenfrequency of the system in which the foundation stiffnesses are replaced by the tangent stiffnesses $\partial F_h/\partial u_0$ and $\partial M_f/\partial\theta$ at time t. Because the tangent stiffness returns to its small-strain value at every unloading, ω_t oscillates from cycle to cycle. The secant-window frequency $\omega_s(t)$ uses the equivalent stiffnesses over the last $T_w = 1$ s,

$$K_{h,s}(t) = \frac{\max\limits_{\tau\in[t-T_w,\,t]} \left|F_h^{\mathrm{hys}}(\tau)\right|}{\max\limits_{\tau\in[t-T_w,\,t]} |u_0(\tau)|} \qquad (6)$$

and the analogous expression for rocking, where F^{hys} is the force of the hysteretic spring without the dashpot. ω_s describes the persistent softening and is used to define the detuning. For a TMD with mass ratio μ, the classical tuning for an undamped primary structure under harmonic force is [1]

$$f_{opt} = \frac{1}{1+\mu}, \qquad \zeta_{opt} = \sqrt{\frac{3\mu}{8(1+\mu)^3}} \qquad (7)$$

and the detuning index is

$$D(t) = \frac{\omega_d(t)}{\omega_s(t)} - f_{opt} \qquad (8)$$

$D = 0$ means that the damper is tuned in the classical sense to the instantaneous system. A passive TMD tuned to the small-strain frequency starts at $D = 0$ and drifts to $D > 0$ as the foundation softens, because ω_s decreases while ω_d stays constant.

3 TMD designs

3.1 Passive designs

Three passive designs share the mass ratio $\mu = 0.02$. P1 is tuned to the fixed-base frequency of the frame, $\omega_d = f_{opt}\omega_{fb}$, with $\zeta_d = \zeta_{opt}$. P2 is tuned to the small-strain soil–structure frequency ω_0, $\omega_d = f_{opt}\omega_0$, with $\zeta_d = \zeta_{opt}$. P3 is optimised numerically: the pair (f_d, ζ_d), with $f_d = \omega_d/\omega_0$, is selected from a candidate set of $f_d \in \{0.70, 0.85, 1.00\}$ and $\zeta_d \in \{0.05, 0.10, 0.20\}$ together with the pair of Eq. (7), by minimising the mean plus one standard deviation of the peak roof displacement over three training motions at the same intensity. All reported results use five different test motions.

3.2 Frequency estimation

Only the roof absolute acceleration y_k, sampled every $\Delta t = 0.01$ s and corrupted by Gaussian noise of 5% of its running RMS value, is assumed to be measured. The signal passes a causal second-order Butterworth band-pass filter from 0.4 to 1.4 times the small-strain frequency. A second-order autoregressive model $y_k = -a_1 y_{k-1} - a_2 y_{k-2} + e_k$ is identified recursively with a forgetting factor $\lambda = 0.985$ [23]:

$$\varphi_k = [-y_{k-1}, -y_{k-2}]^T, \quad G_k = \frac{P_{k-1}\varphi_k}{\lambda + \varphi_k^T P_{k-1}\varphi_k} \qquad (9)$$

$$\hat{\theta}_k = \hat{\theta}_{k-1} + G_k\left(y_k - \varphi_k^T \hat{\theta}_{k-1}\right), \quad P_k = \frac{P_{k-1} - G_k \varphi_k^T P_{k-1}}{\lambda} \qquad (10)$$

with $\hat{\theta} = [\hat{a}_1, \hat{a}_2]^T$. The poles of the identified model give the frequency

$$\hat{\omega}_k = \frac{1}{\Delta t}\arccos\left(\frac{-\hat{a}_1}{2\sqrt{\hat{a}_2}}\right) \qquad (11)$$

which is smoothed by a first-order low-pass filter with a time constant of 0.3 s. Estimates are not used during the first second.

3.3 Retuning law and actuator model

The adaptive TMDs (A: estimated frequency; A*: exact secant-window frequency ω_s from the model) start from the tuning of P2 and command the stiffness

$$k_{cmd}(t) = \mathrm{clip}\left[m_d\left(f_{opt}\,\omega_{use}(t)\right)^2,\ 0.3\,k_{d0},\ 1.1\,k_{d0}\right] \qquad (12)$$

$$\tau_a \dot{k}_d = k_{cmd} - k_d, \quad \left|\dot{k}_d\right| \le R \qquad (13)$$

where ω_{use} is $\hat{\omega}$ for A and ω_s for A*, k_{d0} is the nominal stiffness of P2, $\tau_a = 0.05$ s is the actuator time constant and $R = 2k_{d0}$ per second is the rate limit. The damping coefficient is kept at the value of P2. The device is semi-active: it only needs power to change stiffness, and it fails safe to the passive P2 design.

3.4 Performance measures and statistical comparison

The measures are the peak roof displacement relative to the ground, the peak interstorey drift ratio, the peak TMD stroke and the peak foundation rocking. The reduction of the roof displacement is expressed relative to the uncontrolled frame (U) on the same soil, intensity and motion. Two designs are compared through paired differences per motion, in percentage points of the uncontrolled peak roof displacement, with the mean and the standard deviation over the five test motions per case, and pooled over the eight cases (40 paired comparisons) with a 95% confidence interval of the mean (1.96 standard errors). The 40 comparisons are not fully independent because cases share motions, so the intervals are indicative.

4 Case studies

4.1 Frames

The frames are the shear-type models of the authors' earlier work [19]: a 7-storey and an 11-storey frame with a storey height of 3.2 m (Table 1). The 7-storey frame uses storeys 1–7 of Table 1. The fixed-base fundamental periods are 0.627 s and 0.899 s.

Table 1. *Storey data of the 11-storey frame; the 7-storey frame uses storeys 1–7 with identical values.*

Storey	Mass (kg)	Stiffness (N/m)
1	215 370	4.68×10^8
2	201 750	4.76×10^8
3	201 750	4.68×10^8
4	200 930	4.50×10^8
5	200 930	4.50×10^8
6	200 930	4.50×10^8
7	203 180	4.50×10^8
8	202 910	4.37×10^8
9	202 910	4.37×10^8
10	176 100	4.37×10^8
11	66 230	3.12×10^8

4.2 Soils and foundation

The soft soil uses the sway and rocking stiffnesses and dashpot coefficients of the earlier work [19] (Table 2). The medium soil is a parametric variation in which the stiffnesses are multiplied by 4 (shear-wave velocity doubled) and the dashpot coefficients by 2. The equivalent footing radius $R = 12.1$ m is back-calculated from the ratio of the rocking to the sway stiffness of the soft soil, using the closed forms for a rigid circular footing on an elastic half-space [24] and an assumed Poisson ratio of 0.4. The yield sway and rotation of the springs are set from assumed capacities: a sliding capacity of $0.4W$ and an overturning moment capacity of $0.5WR$ for the soft soil, both multiplied by 1.5 for the medium soil, with W the weight of the frame plus the foundation block. The foundation block has the mass of the first storey and a rotational

inertia of $m_0R^2/4$. These capacities and the medium soil are modelling assumptions of this study, not site data. The resulting small-strain periods with SSI are given in Table 4.

Table 2. *Foundation parameters.*

Soil	K_h (N/m)	K_θ (N m/rad)	c_h (N s/m)	c_θ (N m s/rad)
Soft	1.10×10^{9}	1.43×10^{11}	7.48×10^{7}	2.47×10^{9}
Medium	4.40×10^{9}	5.72×10^{11}	1.50×10^{8}	4.90×10^{9}

4.3 Ground motions and analysis settings

Ground motions are generated as stationary white noise passed through a Kanai–Tajimi filter [25, 26], multiplied by an envelope that rises over 2 s, stays constant until 8 s and decays exponentially with a time constant of 4 s, for a total duration of 16 s. The filter frequency ω_g and damping ratio ζ_g are varied between 9 and 18 rad/s and between 0.5 and 0.6. Three motions (ω_g, ζ_g = 11, 0.5; 15, 0.6; 13, 0.55) are used to select P3 and five other motions (9, 0.5; 13, 0.55; 18, 0.6; 11, 0.6; 16, 0.5) are used for all reported results. Each motion is scaled to a peak ground acceleration of 0.2 g or 0.5 g. The TMD mass ratio is $\mu = 0.02$. All computations were programmed in Python 3.12 with NumPy 2.4 and SciPy 1.17.

5 Verification

The code was verified against independent solutions before the case studies were run (Table 3).

Table 3. *Verification results.*

Check	Result
SSI period elongation of a single-degree-of-freedom system against the closed form of Eq. (5)	relative error 1.8×10^{-10}
7-storey frame with TMD, steady-state TMD amplitude from the time-domain solution against the frequency-response solution (linear case)	relative error 1.6×10^{-4}
Bouc–Wen spring: initial stiffness divided by K, maximum of z	0.9992; 0.9967 (bounded by 1)
Bouc–Wen spring: energy dissipated in one cycle	positive (1.75×10^{5} J in the test cycle)
Frequency estimator on a known chirp from 1.0 to 0.6 Hz, no noise, no band-pass, $\lambda = 0.98$	mean relative error 0.9%
Same chirp, 5% noise, no band-pass	no valid estimate
Same chirp, 5% noise, with band-pass, $\lambda = 0.98$ and 0.995	mean relative error 1.9% and 4.5%

The test with noise shows why the band-pass filter in Section 3.2 is needed. The hysteresis loops have not been compared with cyclic tests of footings; this remains a limitation (Section 7).

6 Results

6.1 Foundation softening

Table 4 gives the periods and the largest drop of the two frequencies of Section 2.5 for the eight cases. The small-strain SSI period of the soft soil is 16.7% (7 storeys) and 19.4% (11 storeys) longer than the fixed-base period, against 5.7% and 6.6% for the medium soil. During the motions, the secant-window frequency fell by 3% to 32% below its small-strain value, the largest drop occurring for the 11-storey frame on the soft soil at 0.5 g. The tangent frequency dropped by up to 46% but recovered at every unloading, as the loops of Fig. 2 and the frequency histories of Fig. 3 show.

Table 4. *Periods and largest drop of the secant-window and tangent frequencies (fraction of the small-strain frequency).*

Frame (storeys)	Soil	PGA (g)	T fixed (s)	T SSI small-strain (s)	Max drop of secant-window frequency (%)	Max drop of tangent frequency (%)
7	medium	0.2	0.627	0.663	3.1	3.1
7	medium	0.5	0.627	0.663	9.0	23.1
7	soft	0.2	0.627	0.732	12.0	11.6
7	soft	0.5	0.627	0.732	23.0	41.1
11	medium	0.2	0.899	0.958	2.6	4.6
11	medium	0.5	0.899	0.958	8.5	27.1
11	soft	0.2	0.899	1.073	16.8	13.9
11	soft	0.5	0.899	1.073	32.5	46.1

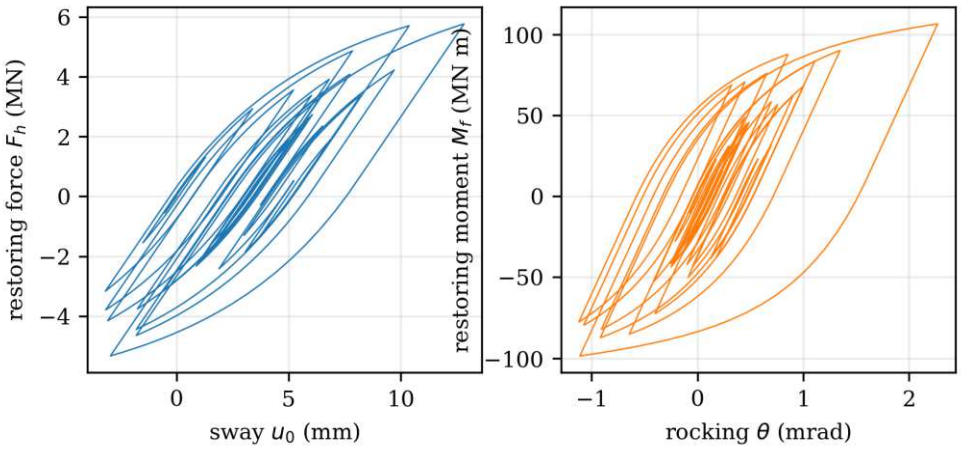


Fig. 2. *Foundation hysteresis of the 7-storey frame on soft soil at 0.5 g, uncontrolled: (left) sway, (right) rocking.*

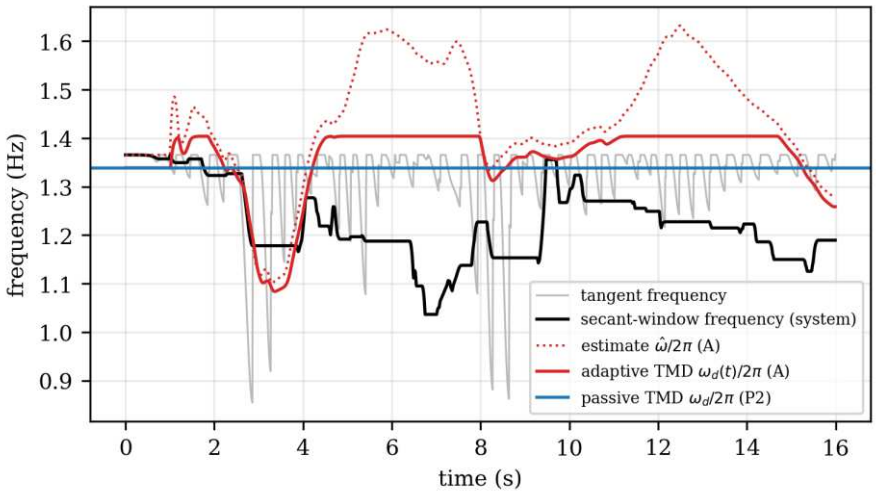


Fig. 3. *Frequency histories for the 7-storey frame on soft soil at 0.5 g: tangent and secant-window frequencies of the system, the estimate and the stiffness-controlled frequency of the adaptive TMD (A), and the frequency of the passive TMD (P2).*

6.2 Passive TMDs

Table 5 and Fig. 4 give the reduction of the peak roof displacement. The TMD tuned to the soil–structure frequency (P2) reduced the roof displacement by 8.3% to 17.0%. Tuning to the fixed-base frequency (P1) was less effective than P2 in all eight cases, and in one case (11 storeys, soft soil, 0.5 g) it increased the response by 3.0% while P2 reduced it by 11.6%. Pooled over the 40 paired comparisons, P2 outperformed P1 by 7.2 percentage points (95% CI ±2.6), and was better in 70% of the comparisons. The optimised passive design (P3) did not improve on P2: on the test motions it was on average 1.3 points worse (±1.4)

and better in only 23% of the comparisons. In four of the eight cases the optimisation selected the pair of Eq. (7) or nearly so (Table 6), and in the 7-storey soft-soil case at 0.2 g it selected a pair that performed poorly on the test motions (7.4% against 15.2% for P2), which indicates over-fitting to three training motions.

Table 5. *Peak roof displacement of the uncontrolled frame (U) and reduction (%) by the five TMD designs (mean of five test motions). P1: fixed-base tuning; P2: small-strain soil–structure tuning; P3: optimised passive; A: adaptive, estimated frequency; A*: adaptive, exact frequency.*

Frame	Soil	PGA (g)	U roof (mm)	P1 red. (%)	P2 red. (%)	P3 red. (%)	A red. (%)	A* red. (%)
7	medium	0.2	59.2	8.2	12.6	12.6	12.1	13.3
7	medium	0.5	134.6	5.0	8.3	7.3	6.9	9.4
7	soft	0.2	57.9	7.5	15.2	7.4	14.8	14.5
7	soft	0.5	133.4	4.6	10.4	6.5	10.5	10.1
11	medium	0.2	93.9	12.0	16.2	16.2	13.4	16.6
11	medium	0.5	212.7	6.1	9.4	9.4	7.1	10.7
11	soft	0.2	96.8	3.0	17.0	18.1	15.8	16.1
11	soft	0.5	225.8	-3.0	11.6	13.1	9.6	10.6

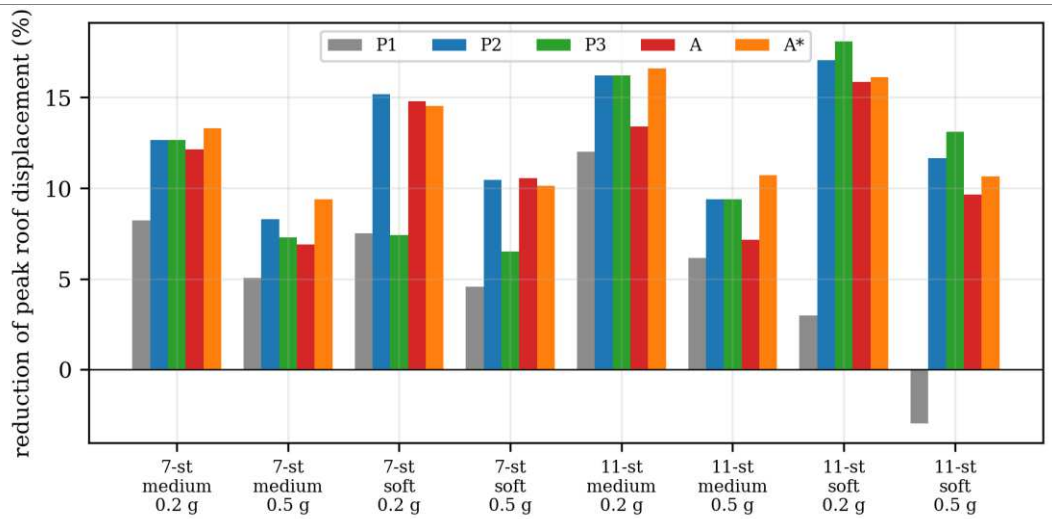


Fig. 4. *Reduction of the peak roof displacement relative to the uncontrolled frame, mean of five test motions.*

Table 6. *Parameters selected for P3, peak TMD stroke and peak foundation rocking.*

Frame	Soil	PGA (g)	P3 f_d/f_s	P3 ζ_d	Stroke P2 (mm)	Stroke P3 (mm)	Stroke A (mm)	Stroke A* (mm)	Rocking U (mrad)	Rocking P2 (mrad)	Rocking A (mrad)
7	medium	0.2	0.98	0.08	183	183	187	182	0.18	0.15	0.15
7	medium	0.5	1.00	0.10	414	377	427	412	0.79	0.65	0.69
7	soft	0.2	0.70	0.20	156	108	157	158	0.60	0.49	0.50
7	soft	0.5	0.70	0.05	326	401	324	348	2.15	1.84	1.85
11	medium	0.2	0.98	0.08	243	243	238	244	0.27	0.22	0.23
11	medium	0.5	0.98	0.08	542	542	529	550	1.29	1.02	1.07
11	soft	0.2	1.00	0.05	239	281	240	244	0.90	0.71	0.73
11	soft	0.5	1.00	0.05	472	556	467	486	3.18	2.58	2.69

6.3 Adaptive retuning

Fig. 5 and Table 7 compare the adaptive designs with P2. The adaptive TMD with the estimated frequency (A) reduced the roof displacement less than P2 in 7 of the eight cases (by 0.4 to 2.8 points in the mean) and equally in the remaining case; pooled, it was 1.3 points worse than P2 (±1.2) and better in 45% of the comparisons. The adaptive TMD with the exact frequency (A*) differed from P2 by -1.0 to +1.3 points in the means of the cases, and pooled the difference was +0.1 points (±0.7), which is not distinguishable from zero. Relative to P3, A differed by 0.0 points (±1.7). The gap between A and A* is due to the estimation

error: the estimate was biased high in parts of the records and reached the upper limit of the stiffness range (Fig. 3).

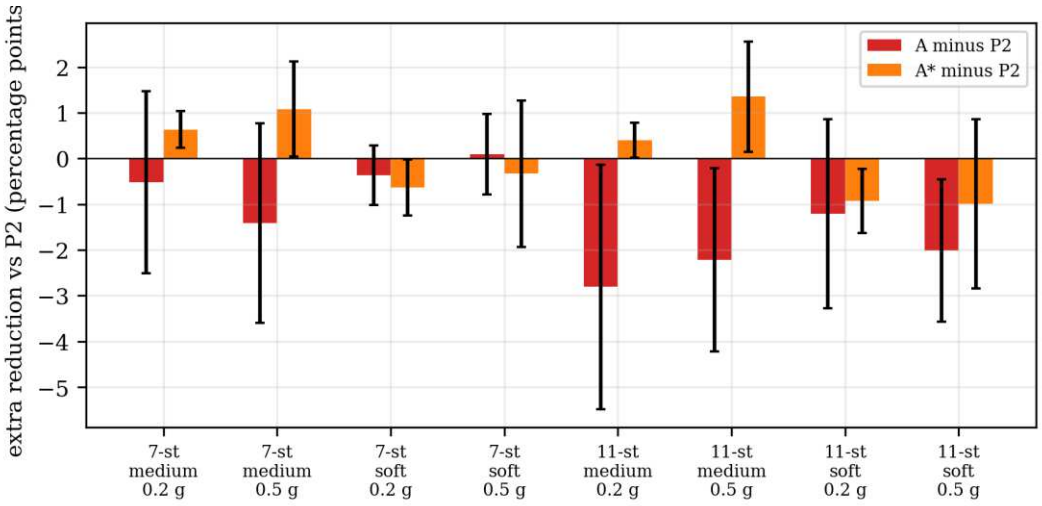


Fig. 5. *Extra reduction of the peak roof displacement by the adaptive designs relative to P2, in percentage points of the uncontrolled response (positive: adaptive better). Bars: mean of five test motions; error bars: standard error.*

Table 7. *Paired difference between the adaptive designs and P2 for each case, in percentage points (mean ± standard deviation over five test motions; positive: adaptive better).*

Frame	Soil	PGA (g)	A minus P2 (pp)	A* minus P2 (pp)
7	medium	0.2	-0.5 ± 4.4	+0.6 ± 0.9
7	medium	0.5	-1.4 ± 4.9	+1.1 ± 2.3
7	soft	0.2	-0.4 ± 1.5	-0.6 ± 1.4
7	soft	0.5	+0.1 ± 2.0	-0.3 ± 3.6
11	medium	0.2	-2.8 ± 6.0	+0.4 ± 0.9
11	medium	0.5	-2.2 ± 4.5	+1.4 ± 2.7
11	soft	0.2	-1.2 ± 4.6	-0.9 ± 1.6
11	soft	0.5	-2.0 ± 3.5	-1.0 ± 4.1

6.4 Detuning index

Fig. 6 shows the detuning index of Eq. (8) for the 7-storey frame on soft soil at 0.5 g. The passive design P2 was detuned by more than 0.1 during 64% of the record, with a maximum of 0.31. The adaptive TMD with the estimated frequency (A) was detuned by more than 0.1 during 65% of the record, with a maximum of 0.37, so the estimator did not reduce the detuning in this case. The adaptive TMD with the exact frequency (A*) stayed close to the classical tuning (mean $|D|$ of 0.004 against 0.117 for P2, and a maximum of 0.07). Despite this large difference in tuning, the peak roof displacement of A* differed little from that of P2 (Table 7).

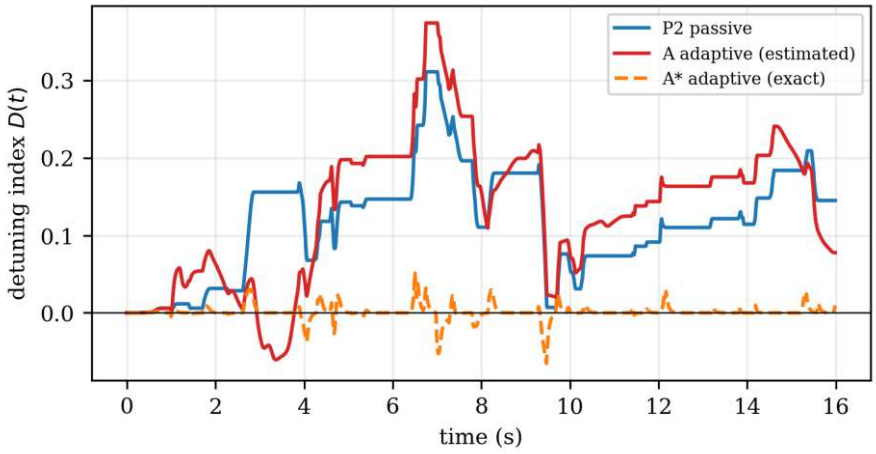


Fig. 6. *Detuning index D(t) for the 7-storey frame on soft soil at 0.5 g.*

6.5 Drift, stroke and rocking

The peak interstorey drift ratio followed the roof displacement (Table 8): the passive design P2 reduced it by 7% to 19% of the uncontrolled value. The peak TMD strokes of the passive and adaptive designs were between 0.11 m and 0.56 m (Table 6), larger than usual for buildings of this height, so the mass ratio and damper properties would need to be revisited for a practical design. The TMD P2 reduced the peak foundation rocking by 14% to 21% (Table 6).

Table 8. *Peak interstorey drift ratio (%).*

Frame	Soil	PGA (g)	U	P1	P2	P3	A	A*
7	medium	0.2	0.34	0.30	0.29	0.29	0.30	0.29
7	medium	0.5	0.77	0.68	0.67	0.68	0.68	0.68
7	soft	0.2	0.27	0.25	0.23	0.25	0.23	0.23
7	soft	0.5	0.55	0.53	0.51	0.53	0.51	0.51
11	medium	0.2	0.39	0.33	0.32	0.32	0.33	0.32
11	medium	0.5	0.81	0.75	0.73	0.73	0.74	0.73
11	soft	0.2	0.28	0.27	0.25	0.25	0.24	0.25
11	soft	0.5	0.57	0.55	0.53	0.53	0.53	0.54

7 Discussion

Soil-aware tuning matters. Tuning the TMD to the soil–structure frequency gave about 7.2 percentage points more reduction of the roof displacement than tuning to the fixed-base frequency, and avoided an amplification of the response on the 11-storey frame on soft soil at 0.5 g. This agrees with the experimental finding that tuning to the soil–structure system improves the damping [8], and with the importance of SSI for TMD design identified in the literature [7, 9]. The reduction by P2 was not smaller on the soft soil than on the medium soil in these models; the peak roof displacement used here includes the rigid-body contribution of the foundation, and the excitation is a broadband stochastic motion, which may explain why the trend reported for stationary random vibration [7] was not seen.

Adaptive retuning did not pay off in these models. The foundation softened substantially, and the passive TMD was detuned in the classical sense during most of the motion. However, the exact adaptive device, which stays tuned, performed like P2, and the realistic adaptive device performed slightly worse.

These results do not prove why. Possible explanations, not tested here, are that the strong phase of the motion is short compared with the time needed to estimate and apply a new tuning, that the tangent softening occurs cycle by cycle and cannot be followed by the damper, and that a TMD with a damping ratio near 0.1 tolerates a mistuning of this size. A study with real motions, longer durations and other mass ratios is needed before this can be generalised.

Practical implication. For frames of this type, designing the TMD with the small-strain stiffness of the foundation, and not the fixed-base frame, captures most of the benefit that was measured, without a sensor, an estimator and an actuator. The optimised passive design on a few training motions was not better than this simple rule.

Limitations. The ground motions are synthetic stochastic motions and not recorded accelerograms, so the conclusions describe trends in these models and not predictions for a site. Only two shear-type frames, two soils, two intensities and one mass ratio were studied, with five test motions per case. The medium soil and the capacities of the foundation springs are assumptions. The macro-element has no uplift, no horizontal–rocking coupling and no pile effects, and its hysteresis has not been compared with cyclic tests of footings such as those used to validate practical nonlinear soil–foundation models [27]. The estimator uses a single sensor with simple noise, the actuator is idealised, and the damping of the adaptive TMD is not changed.

8 Conclusions

1. Under the stochastic motions considered, hysteretic softening of the foundation lowered the secant-window frequency of the frames by 3% to 32% and the tangent frequency by up to 46%, and left a TMD tuned to the small-strain frequency detuned by more than 10% during most of the record in the reference case.

2. Tuning the TMD to the small-strain soil–structure frequency instead of the fixed-base frequency increased the reduction of the peak roof displacement by 7.2 percentage points on average (95% CI ±2.6), and avoided an amplification of the response in one case.

3. A passive design optimised on three training motions was not better than the soil-aware tuning rule on five test motions (1.3 points worse on average).

4. An adaptive variable-stiffness TMD with an estimated frequency reduced the response 1.3 points less than the soil-aware passive design on average, and the same device with the exact frequency was not distinguishable from it (+0.1 points).

5. Within the limits of synthetic motions and two frames, adaptive retuning is not justified over a passive TMD tuned to the soil–structure frequency. The analysis should be repeated with recorded motions and more frames before the result is generalised.

Declarations

Funding [To be completed by the authors: funding statement, or "The authors received no specific funding for this work."]

Competing interests [To be confirmed by the authors: "The authors have no relevant financial or non-financial interests to disclose."]

Author contributions [To be completed by the authors, for example following the CRediT taxonomy.]

Data and code availability The Python code, the storey data, the ground-motion generation settings and the result tables are available [in a public repository: DOI to be added at submission].

Use of AI tools The AI assistant Claude (Anthropic) was used to help draft the manuscript text, to write and test the simulation code and to format the reference list. The authors reviewed the model, the results and the references and take full responsibility for the content.

References

1. Den Hartog JP (1956) Mechanical vibrations, 4th edn. McGraw-Hill, New York
2. Sadek F, Mohraz B, Taylor AW, Chung RM (1997) A method of estimating the parameters of tuned mass dampers for seismic applications. Earthq Eng Struct Dyn 26(6):617–635
3. Rana R, Soong TT (1998) Parametric study and simplified design of tuned mass dampers. Eng Struct 20(3):193–204
4. Veletsos AS, Meek JW (1974) Dynamic behaviour of building-foundation systems. Earthq Eng Struct Dyn 3(2):121–138
5. Mylonakis G, Gazetas G (2000) Seismic soil–structure interaction: beneficial or detrimental?. J Earthq Eng 4(3):277–301
6. NIST (2012) Soil–structure interaction for building structures. NIST GCR 12-917-21. National Institute of Standards and Technology, Gaithersburg, MD
7. Wu J-N, Chen G, Lou M (1999) Seismic effectiveness of tuned mass dampers considering soil–structure interaction. Earthq Eng Struct Dyn 28(11):1219–1233. https://doi.org/10.1002/(SICI)1096-9845(199911)28:11<1219::AID-EQE861>3.0.CO;2-G
8. Jabary RN, Madabhushi SPG (2015) Tuned mass damper effects on the response of multi-storied structures observed in geotechnical centrifuge tests. Soil Dyn Earthq Eng 77:373–380
9. Gorini DN, Chisari C (2022) Impact of soil–structure interaction on the effectiveness of tuned mass dampers. Earthq Eng Struct Dyn 51(6). https://doi.org/10.1002/eqe.3625
10. Wang J-F, Lin C-C (2005) Seismic performance of multiple tuned mass dampers for soil–irregular building interaction systems. Int J Solids Struct 42(20):5536–5554. https://doi.org/10.1016/j.ijsolstr.2005.02.042
11. Farshidianfar A, Soheili S (2013) Ant colony optimization of tuned mass dampers for earthquake oscillations of high-rise structures including soil–structure interaction. Soil Dyn Earthq Eng 51:14–22
12. Golnargesi S, Shariatmadar H, Razavi HM (2018) Seismic control of buildings with active tuned mass damper through interval type-2 fuzzy logic controller including soil–structure interaction. Asian J Civ Eng 19:177–188
13. Masaeli H, Panahi M (2018) Effect of soil and structure nonlinear interaction on the efficiency of tuned mass damper. Civ Eng J 4(10):2474–2490. https://doi.org/10.28991/cej-03091174
14. Ghorbanzadeh M, Sensoy S, Uygar E (2022) Seismic performance assessment of semi active tuned mass damper in an MRF steel building including nonlinear soil-pile-structure interaction. Arab J Sci Eng. https://doi.org/10.1007/s13369-022-07138-0
15. Bakhshinezhad S, Mohebbi M (2020) Multi-objective optimal design of SATMD including soil-structure interaction using NSGA-II. Int J Optim Civ Eng 10(3):391–409
16. Wang L, Shi W, Zhou Y (2022) Adaptive-passive tuned mass damper for structural aseismic protection including soil–structure interaction. Soil Dyn Earthq Eng 158:107298. https://doi.org/10.1016/j.soildyn.2022.107298

17. Nagarajaiah S, Sonmez E (2007) Structures with semiactive variable stiffness single/multiple tuned mass dampers. J Struct Eng 133(1):67–77
18. Nagarajaiah S (2009) Adaptive passive, semiactive, smart tuned mass dampers: identification and control using empirical mode decomposition, Hilbert transform, and short-term Fourier transform. Struct Control Health Monit 16(7–8):800–841
19. Rahmati A (2026) Optimal design of tuned mass dampers in planar frames considering soil flexibility (in Persian). MSc thesis, Faculty of Engineering, Kharazmi University, Tehran, Iran. Supervisor: Shahrouzi M
20. Wen YK (1976) Method for random vibration of hysteretic systems. J Eng Mech Div ASCE 102(2):249–263
21. Ismail M, Ikhouane F, Rodellar J (2009) The hysteresis Bouc-Wen model, a survey. Arch Comput Methods Eng 16(2):161–188
22. Wolf JP (1985) Dynamic soil-structure interaction. Prentice-Hall, Englewood Cliffs, NJ
23. Ljung L (1999) System identification: theory for the user, 2nd edn. Prentice Hall, Upper Saddle River, NJ
24. Gazetas G (1991) Formulas and charts for impedances of surface and embedded foundations. J Geotech Eng 117(9):1363–1381
25. Kanai K (1957) Semi-empirical formula for the seismic characteristics of the ground. Bull Earthq Res Inst Univ Tokyo 35(2):309–325
26. Tajimi H (1960) A statistical method of determining the maximum response of a building structure during an earthquake. In: Proceedings of the 2nd World Conference on Earthquake Engineering, Tokyo and Kyoto, Japan, vol II, pp 781–797
27. Gajan S, Raychowdhury P, Hutchinson TC, Kutter BL, Stewart JP (2010) Application and validation of practical tools for nonlinear soil-foundation interaction analysis. Earthq Spectra 26(1):111–129. https://doi.org/10.1193/1.3263242